

# Characteristic analysis of pulmonary ground-glass lesions with the help of 64-slice CT technology

Y.-G. LV<sup>1</sup>, J.-H. BAO<sup>1</sup>, D.-U. XU<sup>2</sup>, Q.-H. YAN<sup>3</sup>, Y.-J. LI<sup>4</sup>, D.-L. YUAN<sup>1</sup>, J.-H. MA<sup>1</sup>

<sup>1</sup>Medical Imaging Department, Affiliated Hospital of Hebei University of Engineering, Handan, Hebei Province, China

<sup>2</sup>Department of Anatomy, Medical College, Hebei University of Engineering, Handan, Hebei Province, China

<sup>3</sup>Geriatric Medicine, The 1<sup>st</sup> Hospital in Handan, Handan, Hebei Province, China

<sup>4</sup>Medical Imaging Department, Ouzhou County Hospital of Handan, Handan, Hebei Province, China

*Yinggang Lv and Junhui Bao contributed to this work equally*

**Abstract.** – **OBJECTIVE:** With the help of new technologies like 64-slice spiral CT, including latest AW4.4, 2D nodule comparing and analyzing technology, MPR and 3D technology, MIP technology and the technology of analyzing pulmonary vascular density by the method of perfusion scanning, we performed characteristic analysis of ground-glass opacities (GGO) for the early diagnosis of lung cancer.

**PATIENTS AND METHODS:** We selected 62 patients suspected of lung cancer, whose conventional CT showed that they were patients with GGO. With the help of the new technologies of 64-slice spiral CT provided by GE Company, prospective scans were made and 2 to 4 times of review were arranged. After that, the patients were treated with surgery or needle biopsy to get lesion's pathological results. After several scans, the results including lesion's form, density, blood supply, peripheral sign, doubling time and tissue perfusion were drawn to make a comparison. Based on the results, comparative analysis on GGO's characteristics was made from morphological and functional perspectives.

**RESULTS:** 41 patients (66.1%) were pathologically diagnosed with cancer, 10 were diagnosed with inflammation, 7 with fibrosis, and 4 with edema, hemorrhage and other lesions. The comparisons were made between the tumor groups' clinical manifestations (sex, age, symptoms including smoking, coughing, and expectoration), and the difference had no statistical significance ( $p>0.05$ ). Conventional CT scan showed that the shape of GGO was irregular and it showed spiculated sign and pleural indentation. The proportion of the patients with vessel convergence in the tumor group was significantly higher than that of the non-tumor group ( $p<0.05$ ). However, the comparisons between lesions' number, location (superior lobe of the right lung), diameter, edge (blur) and lobulation were made to get a difference ratio ( $p>0.05$ ) which

had no statistical significance. Tumor group's doubling time was significantly short, and its perfusion parameters including BF, BV, MTT, and PS were increased significantly ( $p<0.05$ ).

**CONCLUSIONS:** The new 64-slice CT technology has great value in the diagnosis of the tumorous GGO.

Key Words:

64-slice CT, Maximum intensity projection, Perfusion scan, Vascular density, GGO.

## Introduction

The ground-glass opacities (GGO) is defined as the translucent density area without a certain shape, featuring ill-defined inside lung or easily-defined in the border. Inside this area, textures of blood vessels and bronchial wall are still visible<sup>1</sup>. In addition to inflammatory lesions, bleeding and other non-neoplastic lesions, the diagnosis of peripheral adenocarcinoma, bronchoalveolar carcinoma, atypical adenomatous hyperplasia, and lymphoma can also show the result of GGO<sup>2</sup>. By observing GGO's early density, morphology, growth rate, and changes in infusion blood supply, lesion's nature can be determined. It will provide an appropriate opportunity to remove the early lesions, which is significantly beneficial to the prognosis and the survival rate<sup>3</sup>. Many researchers had tried their best to find the best way to distinguish the changes of ground-glass malignant nodules in a different time. With the help of CT and the difference ratios respectively, the comparative researches were performed on the ground-glass density<sup>4,5</sup>. The comparative

analysis of the manual measurement results of the ground-glass nodule's diameter, volume and quality is also performed<sup>6</sup>. As the wide application and popularization of HRCT and MDCT, more and more ground-glass opacity was found, and its characteristic analysis and clinical value had become a research hot<sup>7</sup>. Especially, the CT perfusion technology boasts about its ability to show the microvascular changes of tumor angiogenesis *in vivo*, which can function in observing the tumor and evaluating its biological activity<sup>8</sup>. The development of PET-CT could provide functional information and molecular metabolic information other than morphology<sup>9</sup>. This information was useful for the diagnosis of lung cancer, staging and therapeutic effects detection<sup>10</sup>.

## Patients and Methods

### Patients

62 patients admitted to our hospital from January of 2015 to January of 2016 were selected. The patients were suspected of lung cancer. The results of their conventional CT showed that they were patients of GGO. Among the patients, 40 were male and 22 were female, with age ranging from 43 to 75 and the average age of  $56.4 \pm 12.3$ . Among them, 28 patients were smokers, 13 had a cough with expectoration, 6 had a fever and 10 had a bloody sputum. The cases diagnosed with tuberculosis, pneumonia, lung surgery, history of wounds, allergy to contrast agents, who cannot cooperatively complete CT enhancement and perfusion scan as well as who got poor quality scan images were excluded. This research got approval from the hospital's Ethnic Committee and informed consent of patients and relatives.

### Methods

#### CT Scanning

Subjects were advised to remove any metal o their body before CT scanning. GE 64-slice CT machine, Medrad® Stellant® CT type high-pressure automatic injector (Malmesbury, Wiltshire, UK), Venofix-19G needle (Braun, Frankfurt, Germany) were applied to train patient's respiration to ensure that patients were breathing evenly. At the end of each patient's breath, 35 seconds of suffocating practice was available. Afterwards, the patients received the conventional chest CT (Siemens, Berlin, Germany) scan, the scan parameter was 120 kV, 200 mAs;

matrix was  $512 \times 512$ ; scanning time was 0.55 s/circuit; collimator was 0.625 m; pitch was 0.89, FOV 360 mm; scanning thickness was 2.5 mm; reconstruction slice thickness was 0.625 mm. The scan ranged from the thoracic entrance to the angle plane of the bilateral rib. After the scan, the data of the location of ground-glass lesions and lesion's morphological feature were obtained. Then, the data was transferred to the workstation to do nodules analysis according to GGO's decision criterion which was that the lesion's maximum diameter should be more than 10 mm and the short burr as well as the lobulated and the vacuole sign should be detected.

Next, with movie perfusion scan mode of CT machine was used to perform perfusion scan and the scanning range was 8 cm of lesions. At a flow rate of 5 ml/s, 50 ml nonionic contrast agent (iopamidol, 300 mg/ml) was intravenously injected with the help of a high-pressure syringe. After 5 seconds of the intravenous injection, the 12 perfusion scans were performed. The interval between two scans was 5 seconds, and the 12 perfusion scans last for 55 seconds. The same scan parameters as the former ones were introduced, 8 perfusion layers were needed, and their thickness was 5 mm or 2.5 mm each. The coverage area of axis Z should cover the entire lesion and a whole tumor perfusion scan was performed to reestablish image in accordance with the conventional standard algorithm (window width 350 HU, window level 40 HU). The scan applies the discontinuous breath scanning methods with different intervals including 1-20s, 28-48s, 56-76s, and 84-104s. Then, the body tumor perfusion analysis software was used to analyze the lesions to get four perfusion parameters which included BF, BV, MTT, and PS. The scanning procedures and methods of review were the same of the first visit. Then, the comparative analyses were done respectively by two senior doctors.

After the perfusion scan, 50 ml contrast agent was injected at a pace of 3.0 ml/s with the help of a high-pressure syringe. Then, the conventional scan was done and the scan parameters were also as same as the former ones. With the help of the latest software of version AW4.4 (perfusion software, nodules comparative analysis software, 2D and 3D reconstruction software and MIP technology, etc.), the perfusion scan images were transmitted to the workstation. The principles of the formation of perfusion scan images were drawn from radio-

**Table I.** Characteristic analysis of the conventionally scanned ground-glass lesion.

Group	Number of cases	Number of lesions	Position (right upper the lobe)	Diameter (mm)	Shape (irregular)	Edge (Fuzzy)	Spicule sign	Leaf	Pleural indentation and convergence vascular sign
Tumor	41	1.2±0.4	23 (56.1)	15.5±4.2	25 (61.0)	24 (58.5)	21 (51.2)	16 (39.0)	14 (34.1)
Non-tumor	21	0.9±0.3	9 (42.9)	13.4±4.5	7 (33.3)	10 (47.6)	5 (23.8)	8 (38.1)	2 (9.5)
<i>t</i> ( $\chi^2$ )		0.326	0.975	0.632	4.249	0.668	4.285	0.005	4.397
<i>p</i>		0.411	0.323	0.548	0.039	0.414	0.038	0.943	0.036

tracer dilution principles and laws of the central volume which belong to the research area of nuclear medicine. According to the protocol of perfusion scanning, Mode “cine” perfusion scan of CT machine was introduced. According to the enhanced image and blood volume’s color graphic, the maximum layer of the tumor was chosen to serve as analyzing and calculating layer. ROI was also be set on the lumps and aorta, and the maximum cross-sectional area was greater than 60%-70% of the maximum sectional area of the tumor. Meantime, attention was given to avoid partial volume effects.

#### *Pathological Evaluation*

Pathological samples were obtained by surgery or needle biopsy for H & E and reticular endothelial staining. Through pathological exam, the lesion’s nature was decided and its histological features were grabbed.

#### *Statistical Analysis*

SPSS 19.0 (IBM Corporation, Armonk, NY, USA) statistical software was used for statistical analysis and data were expressed as mean  $\pm$  standard deviation. The comparison between groups was made by *t*-test. The enumeration data were expressed by percentage (%). The comparison between groups was made by  $\chi^2$ -test.  $p < 0.05$  was considered to be statistically significant.

## Results

### *Clinical Manifestations and Characteristic Analysis of Conventional Scanning*

After pathological diagnosis, 41 patients (61%) were diagnosed with cancer among which 20 were diagnosed with bronchoalveolar carcinoma, 12 were peripheral adenocarcinoma, 9 were atypical adenomatous hyperplasia, 10 were in-

flammation, 7 were fibrosis, and 4 were edema, hemorrhage, and other lesions. The comparison between clinical manifestations (sex, age, symptoms of smoking, coughing and expectoration) showed that the difference ratio ( $p > 0.05$ ) had no statistical significance. Conventional CT scan showed that the shape of GGO was irregular and it showed speculated sign and pleural indentation. The proportion of the patients with vessel convergence in tumor group was significantly higher than that of the non-tumor group ( $p < 0.05$ ). However, the comparisons between lesions’ number, location (superior lobe of the right lung), diameter, edge (blur) and lobulation were made to get a difference ratio ( $p > 0.05$ ) which had no statistical significance (Table I and Figure 1).

### *Comparison of Perfusion Scans of the Ground-glass Lesions*

The doubling time of the tumor group was significantly short, the perfusion parameters of BF, BV, MTT, and PS were also significantly increased ( $p < 0.05$ ) (Table II and Figure 1).

## Discussion

The change of the lung’s density resulted in the formation of ground-glass opacity, and the volume of pulmonary blood, the volume of pulmonary extravascular fluid, the density of the inherent lung tissue, and the density of the lungs chamber constituted the lung’s density. Any disease which causes the above factors would lead to the formation of the ground-glass opacity<sup>11</sup>. The lung’s ground-glass shadow would appear under such circumstances including hyperplasia of the alveolar wall columnar cell, an increase of cell density, gas filling of part of the alveoli and terminal airbags due to the reduce of lung’s actual air content and the incomplete collapse of alveoli<sup>12</sup>. The pathological types including lung tissue portion

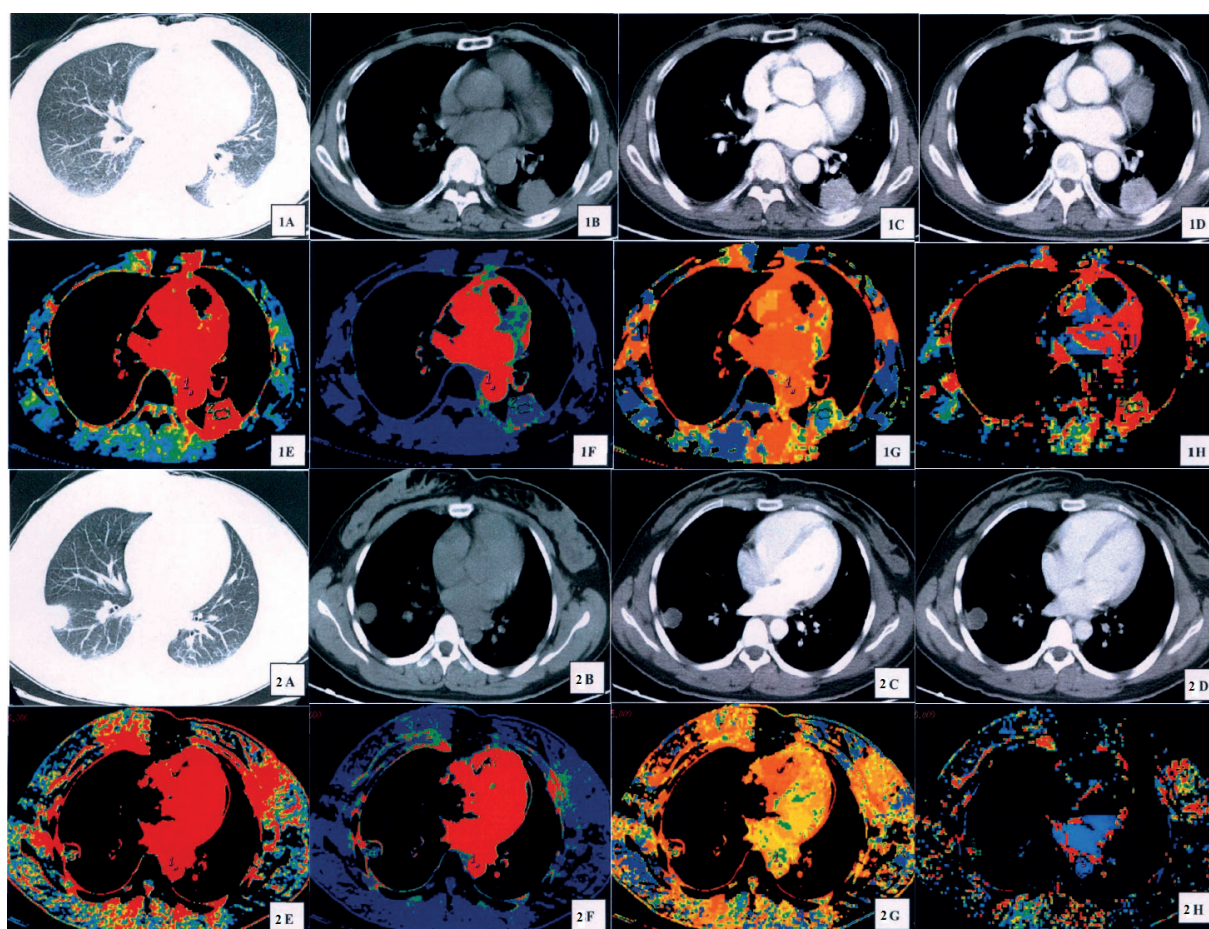


**Figure 1.** CT perfusion scan of ground-glass lesions (1A-1H shows adenocarcinoma. *A-D* is plain scan and enhanced diagram, which shows multiple small burr edge of the lesions, and moderate homogeneous enhancement. *E-H* is the perfusion parameter program, and the peripheral lesion is hypertransfusion, and its center is hypoperfusion. *E* is the graph of BV, and its value is 11.2 ml/100 g. *F* is the graph of BF, and its value is 125.4 ml/min · 100 g. *G* is the graph of MTT, and its value is 10.3s. *H* is the graph of PS, and its value is 17.6 ml/min · 100 g. 2 *A-H* shows the recovering period of pneumonia. *A-D* is plain and enhanced diagrams, which shows the edge of the lesion is finishing, and the reinforcement is not obvious. *E-H* is the perfusion parameter program, and most of the parts are low density areas. *E* is the graph of BV, and its value is 5.3 ml/100 g. *F* is the graph of BF, and its value is 26.2 ml/min · 100 g. *G* is the graph of MTT, and its value is 4.4s. *H* is the graph of PS, and its value is 1.9 ml/min · 100 g).

**Table II.** Comparison of perfusion scan of the ground-glass lesions.

Group	Doubling time (d)	BF (ml/min·100 g)	BV (ml/100 g)	MTT(s)	PS (ml/min·100 g)
Tumor	136.4±42.2	116.3±32.5	14.6±3.7	13.9±4.6	22.1±6.6
Non-tumor	213.5±53.1	46.7±18.2	5.8±1.4	7.7±2.2	4.3±1.2
T ( $\chi^2$ )	10.325	8.965	9.432	12.632	15.847
p	<0.001	<0.001	<0.001	<0.001	<0.001

Note: BF, blood flow volume; BV, blood volume; MTT, mean transit time; PS, permeability of surface.

exudative, tumor cell infiltration, interstitial inflammatory thickening, fibrosis, edema, etc.<sup>13</sup>. In the interstitial-based lesions, the diffused ground-glass opacity was more common<sup>14</sup>. In the sub-

stantive-based lesions, the ground-glass opacity's boundary was more clear, and it appears circumscript or in diffuse distribution, and it might be associated with pulmonary consolidation shadows<sup>15</sup>.

The ground-glass opacity and lung adenocarcinoma *in situ* were closely related to the pathology, and the prognosis of the patients with lung cancer could be assessed by measuring the diameter of the ground-glass opacity on HRCT<sup>16,17</sup>. The GGO area measured on HRCT had a good effect on the assessment of pulmonary adenocarcinoma patient's overall survival period and relapse-free survival period, and the GGO ratio might be the independent factor which could affect the prognosis of the lung's small gland adenocarcinoma<sup>18</sup>.

When the GGO whose diameter more than 15 mm showed nodules or showed high-pixel attenuation, it was more inclined to be the invasive adenocarcinoma<sup>19</sup>. CT perfusion imaging technique was a quantitative research method which was economical and practical without the use of radionuclides, and its images' space and time definition were high, and its scanning device was simple, less affected and time shortened. Perfusion imaging techniques had a great advantage for the study of tissue and organ hemodynamics, and its effectiveness repeatability had been confirmed by the basic research and clinical applications. Currently, lung CT perfusion imaging technique was one of the most convenient, efficient and practical tools to the quantitative research of lung tissue blood perfusion. At the same time, lung CT perfusion imaging could obtain the anatomy image of high-density resolution anatomical images and high spatial resolution, so it had a very good development prospects. It could be generalized from the research that the conventional CT scan showed the formation of tumor group's ground-glass lesions (irregular shape), the burr and the pleural indentation vascular, and the vessel convergence sign ratio was significantly more than the non-cancer group. But the comparison of the number of lesions, location (on the right lung leaf), diameter, edge (blur) and lobulation sign, and the difference had no statistical significance. The doubling time of the tumor group was short, the perfusion parameters of BF, BV, MTT, and PS were increased, and the difference had statistical significance.

The problems of lung CT perfusion imaging were 1) Currently CT respiratory gating machine cannot yet be connected with the scanning sequence, so the patient's respiration training effect can affect the success of the perfusion; 2) Intermittent breath scanning will lose part of the time's scanning data, so the selection of periods of time needs the pre-trial and repeatedly grope; 3) Determination of the threshold value of the

perfusion scan has no experience can learn; 4) On the perfusion level, the selection of ROI entirely depends on the operator's experience, so it lacks consistency. At the same time, expanding the sample size and analyzing the different tumor lesions such as adenocarcinoma, squamous carcinoma, and other features has important reference value to early diagnosis of tumors and guidance of clinical treatment.

## Conclusions

We observed that the new 64-slice CT technology has great value for the early diagnosis of lung cancer GGO.

## Acknowledgments

This study was supported by the Hebei province Science and Technology Support Project (No: 12276104D-19), Medical Science Research Key Project of Hebei province (No: 20090188) and Science and Technology Research and Development Project of Handan city (No: 0923108054-5).

## Conflict of interest

The authors declare no conflicts of interest.

## References

- 1) MIURA A, AKAGI S, NAKAMURA K, OHTA-OGO K, HASHIMOTO K, NAGASE S, KOHNO K, KUSANO K, OGAWA A, MATSUBARA H, TOYOOKA S, OTO T, OHTSUKA A, OHE T, ITO H. Different sizes of centrilobular ground-glass opacities in chest high-resolution computed tomography of patients with pulmonary veno-occlusive disease and patients with pulmonary capillary hemangiomatosis. *Cardiovasc Pathol* 2013; 22: 287-293.
- 2) KIM HY, SHIM YM, LEE KS, HAN J, YI CA, KIM YK. Persistent pulmonary nodular ground-glass opacity at thin-section CT: histopathologic comparisons. *Radiology* 2007; 245: 267-275.
- 3) PARK JH, LEE KS, KIM JH, SHIM YM, KIM J, CHOI YS, YI CA. Malignant pure pulmonary ground-glass opacity nodules: prognostic implications. *Korean J Radiol* 2009; 10: 12-20.
- 4) NOMORI H, YAMASHITA Y, ODA S, AWAI K, LIU D, NAKAURA T, YANAGA Y. Ground-glass opacities on thin-section helical CT: differentiation between bronchiole alveolar carcinoma and atypical adenomatous hyperplasia. *AJR Am J Roentgenol* 2008; 190: 1363-1368.
- 5) HIGUCHI K, NAGAO M, MATSUI Y, SUNAMI S, KAMITANI T, JINNOUCHI M, YONEZAWA M, YAMASAKI Y, YABUUCHI H,

- HATKENAKA M, HONDA H. Detection of ground-glass opacities by use of hybrid iterative reconstruction (iDose) and low-dose 256-section computed tomography: a phantom study. *Radiol Phys Technol* 2013; 6: 299-304.
- 6) GIETEMA H, NOSSENT G, SCHAEFER-PROKOP C, VAN DE VORST S, PROKOP M, STARING M, PLUIM JP, DE HOOP B, KLEIN S, VAN GINNEKEN B. Image subtraction facilitates assessment of volume and density change in ground-glass opacities in chest CT. *Invest Radiol* 2009; 44: 61-66.
  - 7) ICHINOSE J, KOHNO T, FUJIMORI S, HARANO T, SUZUKI S, FUJII T. Invasiveness and malignant potential of pulmonary lesions presenting as pure ground-glass opacities. *Ann Thorac Cardiovasc Surg* 2014; 20: 347-352.
  - 8) PONTANA F, REMY-JARDIN M, DUHAMEL A, FAIVRE JB, WALLAERT B, REMY J. Lung perfusion with dual-energy multi-detector row CT: can it help recognize ground-glass opacities of vascular origin? *Acad Radiol* 2010; 17: 587-594.
  - 9) WANG GM, LIU DF, XU YP, MENG T, ZHU F. PET/CT imaging in diagnosing lymph node metastasis of esophageal carcinoma and its comparison with pathological findings. *Eur Rev Med Pharmacol Sci* 2016; 20: 1495-1500.
  - 10) FISCHER BM, MORTENSEN J. The future in diagnosis and staging of lung cancer: Positron emission tomography. *Respiration* 2006; 73: 267-276.
  - 11) MAO H, LABH K, HAN F, JIANG S, YANG Y, SUN X. Diagnosis of the invasiveness of lung adenocarcinoma manifesting as ground-glass opacities on high-resolution computed tomography. *Thorac Cancer* 2016; 7: 129-135.
  - 12) LIM E, NICHOLSON AG, PADLEY S, POPAT S. Never smoker with ground-glass opacities on CT. *Lancet Respir Med* 2015; 3: 328.
  - 13) KALCHIEM-DEKEL O, MAIMON N, SHACK AR, SMOLIAKOV A, SHACO-LEVY R, FRUCHTER O, FOX BD, KRAMER MR, GALANTE O. An unusual presentation of malignant melanoma metastatic to the lungs and bronchi. Bilateral ground-glass opacities with a "crazy paving" component. *Am J Respir Crit Care Med* 2015; 191: 954-955.
  - 14) CREQUIT P, WISLEZ M, FLEURY FJ, ROZENSZTAJN N, JABOT L, FRIARD S, LAVOLE A, GOUNANT V, FILLON J, ANTOINE M, CADRANEL J. Crizotinib associated with Ground-Glass opacity predominant pattern interstitial lung disease: a retrospective observational cohort study with a systematic literature review. *J Thorac Oncol* 2015; 10: 1148-1155.
  - 15) SHIMADA Y, SAJI H, OTANI K, MAEHARA S, MAEDA J, YOSHIDA K, KATO Y, HAGIWARA M, KAKIHANA M, KAJIWARA N, OHIRA T, AKATA S, IKEDA N. Survival of a surgical series of lung cancer patients with synchronous multiple ground-glass opacities, and the management of their residual lesions. *Lung Cancer* 2015; 88: 174-180.
  - 16) NAKAMURA S, FUKUI T, TANIGUCHI T, USAMI N, KAWAGUCHI K, ISHIGURO F, HIRAKAWA A, YOKOI K. Prognostic impact of tumor size eliminating the ground-glass opacity component: modified clinical T descriptors of the tumor, node, metastasis classification of lung cancer. *J Thorac Oncol* 2013; 8: 1551-1557.
  - 17) DE LUCA N, CAPUZI P, D'ANGELI AL, D'ANTONI L, PAVONE P, DE SANTIS M, DI GIROLAMO M, CATALANO C, PASSARIELLO R. High resolution computed tomography (HRCT) assessment of beta 2-agonist induced bronchodilation in chronic obstructive pulmonary disease patients. *Eur Rev Med Pharmacol Sci* 1999; 3: 83-87.
  - 18) MIAO XH, YAO YW, YUAN DM, LV YL, ZHAN P, LV TF, LIU HB, SONG Y. Prognostic value of the ratio of ground-glass opacity on computed tomography in small lung adenocarcinoma: a meta-analysis. *J Thorac Dis* 2012; 4: 265-271.
  - 19) LEE HY, CHOI YL, LEE KS, HAN J, ZO JI, SHIM YM, MOON JW. Pure ground-glass opacity neoplastic lung nodules: histopathology, imaging, and management. *AJR Am J Roentgenol* 2014; 202: W224-W233.